

**Revisiting the Recommended
Geometry for the Diametrically Compressed
Ceramic C-Ring Specimen**

Osama M. Jadaan
College of Engineering, Mathematics, and Science
University of Wisconsin-Platteville
Platteville, WI 53818
jadaan@uwplatt.edu

Andrew A. Wereszczak
Ceramic Science and Technology Group
Materials Science and Technology Division
Oak Ridge National Laboratory
Oak Ridge, TN 37831-6068
wereszczakaa@ornl.gov

Publication Date: April 2009

Prepared by the
OAK RIDGE NATIONAL LABORATORY
Oak Ridge, Tennessee 37831
managed by
UT-BATTELLE, LLC
for the
U.S. DEPARTMENT OF ENERGY
Under contract DE-AC05-00OR22725

DOCUMENT AVAILABILITY

Reports produced after January 1, 1996, are generally available free via the U.S. Department of Energy (DOE) Information Bridge:

Web site: <http://www.osti.gov/bridge>

Reports produced before January 1, 1996, may be purchased by members of the public from the following source:

National Technical Information Service
5285 Port Royal Road
Springfield, VA 22161
Telephone: 703-605-6000 (1-800-553-6847)
TDD: 703-487-4639
Fax: 703-605-6900
E-mail: info@ntis.fedworld.gov
Web site: <http://www.ntis.gov/support/ordernowabout.htm>

Reports are available to DOE employees, DOE contractors, Energy Technology Data Exchange (ETDE) representatives, and International Nuclear Information System (INIS) representatives from the following source:

Office of Scientific and Technical Information
P.O. Box 62
Oak Ridge, TN 37831
Telephone: 865-576-8401
Fax: 865-576-5728
E-mail: reports@osti.gov
Web site: <http://www.osti.gov/contact.html>

This report was prepared as an account of work sponsored by an agency of the United States Government. Neither the United States government nor any agency thereof, nor any of their employees, makes any warranty, express or implied, or assumes any legal liability or responsibility for the accuracy, completeness, or usefulness of any information, apparatus, product, or process disclosed, or represents that its use would not infringe privately owned rights. Reference herein to any specific commercial product, process, or service by trade name, trademark, manufacturer, or otherwise, does not necessarily constitute or imply its endorsement, recommendation, or favoring by the United States Government or any agency thereof. The views and opinions of authors expressed herein do not necessarily state or reflect those of the United States Government or any agency thereof.

TABLE OF CONTENTS

| | Page |
|--------------------------------------|-------------|
| LIST OF FIGURES | iv |
| LIST OF TABLES | iv |
| ABSTRACT | 1 |
| 1. INTRODUCTION | 2 |
| 2. C-RING STRESS DETERMINATION | 2 |
| 3. EFFECT OF GEOMETRY | 8 |
| 4. RECOMMENDATIONS | 15 |
| 5. ACKNOWLEDGEMENTS | 15 |
| 6. REFERENCES | 16 |

LIST OF FIGURES

| Figure | Page |
|---|------|
| 1. Schematic of the C-ring specimen. | 3 |
| 2. Comparison between the elasticity and mechanics solutions for the C-ring specimen as function of inner to outer radii ratio. | 7 |
| 3. Maximum circumferential tensile stress as function of specimen geometry (adopted from Ref. 2). | 7 |
| 4. One-quarter quarter symmetric model for four of the 20 C-ring geometries considered in this study. The width in the figures is half of the actual C-ring width (symmetry). | 9 |
| 5. Mesh distribution of ANSYS Solid95 type elements. | 9 |
| 6. Hoop stress distribution in the C-ring. Note that the maximum hoop stress occurs at the edge of the specimen. | 10 |
| 7. % difference between mechanics solution and FEA for maximum hoop stress value as function of r_i/r_o and b/t | 12 |
| 8. Stress uniaxiality ratio (σ_θ/σ_z) as function of b/t and r_i/r_o | 13 |
| 9. Absolute value of the stress uniaxiality ratio (σ_θ/σ_z) as function of b/t and r_i/r_o . The scale for the uniaxiality ratio is zoomed in to highlight the demarcation below and above a value of 10. | 14 |
| 10. Ratio of edge hoop stress to center hoop stress at 3-o'clock position of outer surface as function of b/t and r_i/r_o | 15 |

LIST OF TABLES

| Table | Page |
|--|------|
| I. Simulation matrix and FEA results for various C-ring geometries. | 11 |

ABSTRACT

A study conducted several years ago found that a stated allowable width/thickness (b/t) ratio in ASTM C1323 (Standard Test Method for Ultimate Strength of Advanced Ceramics with Diametrically Compressed C-Ring Specimens at Ambient Temperature) could ultimately cause the prediction of a non-conservative probability of survival when the measured C-ring strength was scaled to a different size. Because of that problem, this study sought to reevaluate the stress state and geometry of the C-ring specimen and suggest changes to ASTM C1323 that would resolve that issue. Elasticity, mechanics of materials, and finite element solutions were revisited with the C-ring geometry. To avoid the introduction of more than 2% error, it was determined that the C-ring width/thickness (b/t) ratio should range between 1-3 and that its inner radius/outer radius (r_i/r_o) ratio should range between 0.50-0.95. ASTM C1323 presently allows for b/t to be as large as 4 so that ratio should be reduced to 3.

1. INTRODUCTION

The ASTM Standard Test Method for Ultimate Strength of Advanced Ceramics with Diametrically Compressed C-Ring Specimens at Ambient Temperature [1] has been available for over 10 years. However, a study conducted several years ago [2] found that a stated allowable width/thickness (b/t) ratio in that standard could ultimately lead to non-conservative probability of survival when the measured C-ring strength was scaled to a different size. That is problematic and deserves remedy.

The objective of this study was to reevaluate the stress state and geometry of the C-ring specimen, and suggest changes to ASTM C1323 that would resolve what was observed in Ref. 2. The primary issues investigated were:

- 1) which C-ring stress formula or numerical technique to use in the standard? and
- 2) what geometric boundaries (inner to outer radii ratio, r_i/r_o , and width to thickness ratio, b/t) would desirably maintain hoop stress uniaxiality, and uniformity along specimen width?

2. C-Ring Stress Determination

In general there are three approaches to compute the stress state in a C-ring specimen (geometry shown in Fig. 1). These are:

- "Elasticity" solution as described Timoshenko and Goodier [3],
- "Mechanics of materials" solution using curved beam theory [4-5], and
- Finite element analysis (FEA) method.

What differences exist between the elasticity and mechanics of materials solutions? Both have closed form solutions for the C-ring geometry. An effective way to examine any difference is to explore how they deviate as a function of r_i/r_o . It is important to note that in reality two geometric parameters, r_i/r_o and b/t , affect the stress state in a C-ring. However, the elasticity and mechanics solutions assume the specimen to be narrow; namely, under plane stress condition. In other words, these two approaches predict the stress distribution to be independent of the width, b . Of course the magnitude of the stress would scale linearly with b , but the distribution will remain unchanged. A plane stress condition also means that the stress along the axial direction (width) of the specimen, σ_z , is assumed to be zero.

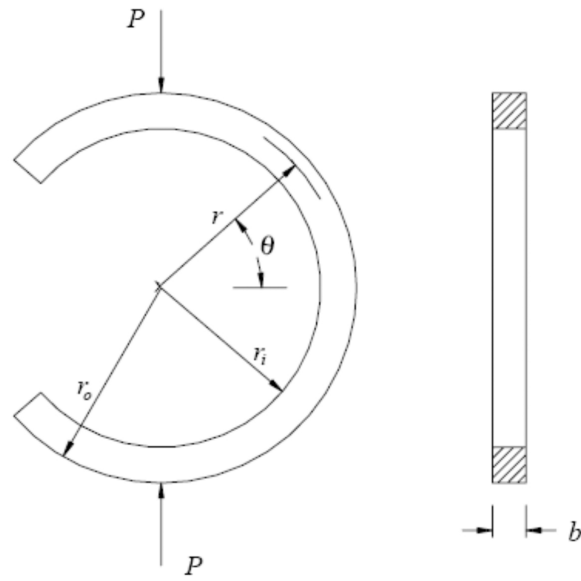


Figure 1. Schematic of the C-ring specimen. P is the compressive force, r_o is the outer radius and r_i is the inner radius, and b is the width. Thickness, t , is $r_o - r_i$.

The elasticity solution describes the stress state in a diametrically compressed C-ring as follows [3]:

$$\begin{aligned}
\sigma_r &= \left(2Ar - \frac{2B}{r^3} + \frac{D}{r}\right) \sin\beta \\
\sigma_\theta &= \left(6Ar + \frac{2B}{r^3} + \frac{D}{r}\right) \sin\beta & \sigma_z &= 0 \\
\tau_{r\theta} &= -\left(2Ar - \frac{2B}{r^3} + \frac{D}{r}\right) \cos\beta \\
A &= \frac{P}{2N} & B &= \frac{-P r_i^2 r_o^2}{2N} & D &= \frac{-P}{N} (r_i^2 + r_o^2) \\
N &= r_i^2 - r_o^2 + (r_i^2 + r_o^2) \ln\left(\frac{r_o}{r_i}\right) \\
\sigma_{\theta, \max} &= \frac{P}{N} \left[3r_o - \frac{r_i^2}{r_o} - \frac{r_i^2 + r_o^2}{r_o} \right] \\
\beta &= 90 - \theta
\end{aligned} \tag{1}$$

where P is the load per unit width.

The mechanics of materials solution describes the stress state in a diametrically compressed C-ring as follows [4-5]:

$$\begin{aligned}
 \sigma_r = \sigma_z &= 0 \\
 P &= \text{Load} \\
 \sigma_\theta &= \frac{PR}{btr} \left[\frac{r - r_a}{r_a - R} \right] \cos \theta & t &= r_o - r_i \\
 R &= \frac{r_o - r_i}{\ln\left(\frac{r_o}{r_i}\right)} & r_a &= \frac{r_o + r_i}{2} \tag{2} \\
 \sigma_{\theta, \max} &= \frac{PR}{btr_o} \left[\frac{r_o - r_a}{r_a - R} \right]
 \end{aligned}$$

Summarizing the elasticity and mechanics of materials solutions:

- The elasticity solution assumes a biaxial stress state in the C-ring where both hoop stress and radial stress (σ_r) components may exist in the C-ring, along with shear stress.
- The mechanics of materials solution assumes the radial stress component to be zero.
- Both approaches assume the axial stress along specimen width to vanish ($\sigma_z=0$).

The following contrasts the elasticity and mechanics of materials solutions:

- 1) Both approaches neglect the axial stress along the width of the C-ring specimen (z-direction). This is because the specimen is assumed to have a narrow (small width) rectangular cross section, resulting in a 2-D (biaxial) stress state.
- 2) Since both the elasticity and mechanics of materials solutions are based on 2-D plane stress analyses, they do not account for the effect of the C-ring width on the stress state as it transitions from plane stress to plane strain condition.
- 3) The elasticity and mechanics of materials hoop stress solutions throughout the specimen, including the maximum stress location, are within 2% of each other for C-rings with $r_i/r_o > 0.53$ (see Fig. 2). The elasticity solution always yields higher circumferential stress than the mechanics of materials solution.
- 4) As can be seen in Fig. 2, as the r_i/r_o ratio decreases (increasing thickness), the discrepancy between the elasticity and mechanics of materials solutions increases. For example, the difference between the two maximum stress solutions reaches 5.4% for $r_i/r_o = 1/3$.
- 5) Hence, it would be constructive if ASTM C1323 [1] delineated an r_i/r_o ratio threshold above which the mechanics of materials solution should be used and below which the elasticity solution should be used. A 2% difference was sought as a threshold error in this study. Therefore, in order to use the mechanics of materials solution with confidence that the maximum stress value is within 2% of the maximum stress of the (more accurate) elasticity solution, then $r_i/r_o > 0.53$.
- 6) The advantages for using the mechanics of materials solution include simplicity, already-derived effective size formulas, and being more conservative (predicting lower stress at failure) compared to the elasticity solution. In addition, Fig. 3 taken from Duffy *et. al.* [2] shows the mechanics of materials solution resulting in a closer maximum stress value to the FEA simulation at the center of the specimen's width (compared to that of the elasticity solution).
- 7) As will be seen later, geometric considerations will lead to recommending that r_i/r_o be greater than 0.50. Thus, as long as $r_i/r_o > 0.50$, the mechanics of materials solution is probably more appropriate for use in ASTM C1323.
- 8) For cases where $r_i/r_o < 0.50$, it is recommended that FEA be utilized because (as will be discussed later) stress uniaxiality is no longer maintained in the specimen.

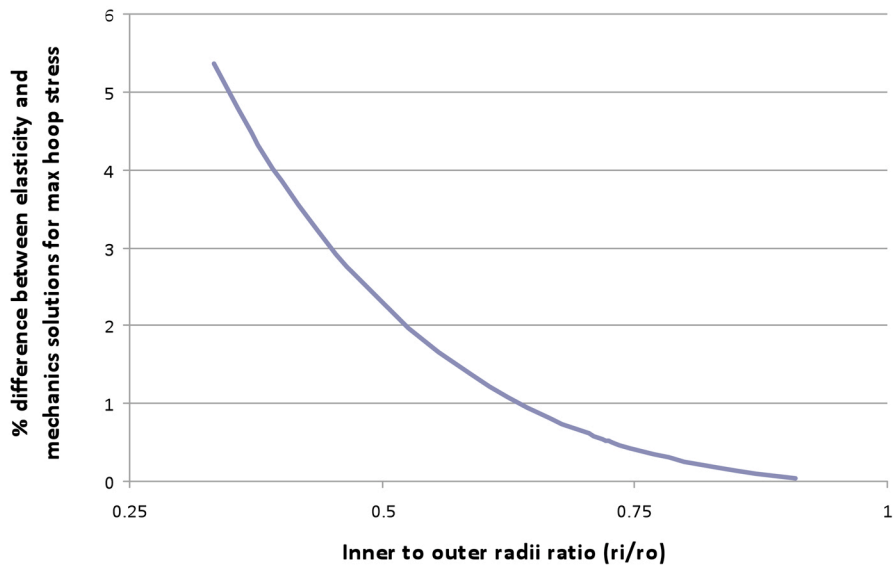


Figure 2. Comparison between the elasticity and mechanics solutions for the C-ring specimen as function of inner to outer radii ratio (r_i/r_o).

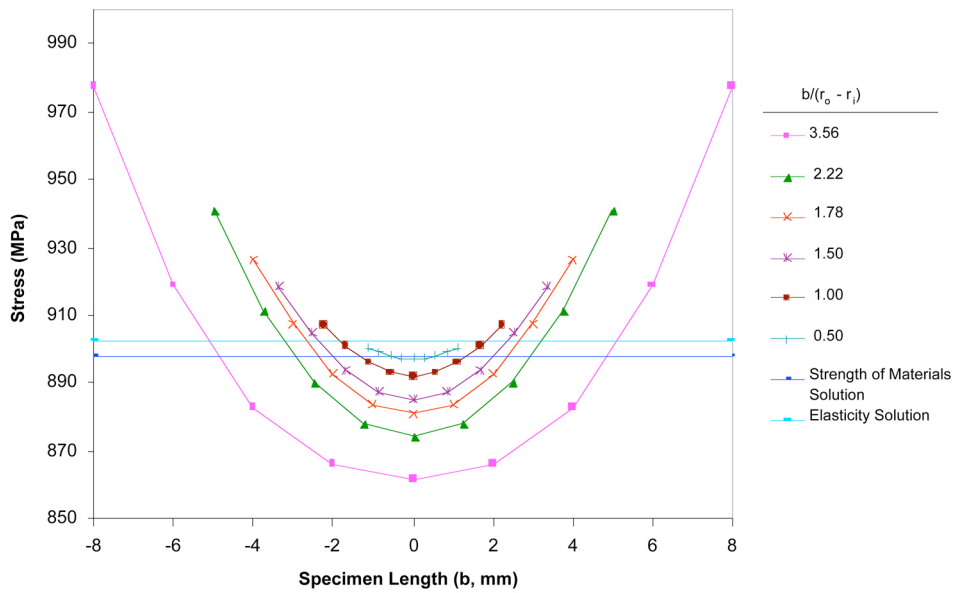


Figure 3. Maximum circumferential tensile stress as function of specimen geometry (from Ref. 2).

3. EFFECT OF GEOMETRY

Unlike the closed form solutions, FEA has the advantage of modeling the 3-D stress state in the C-ring taking into account the effects of both geometric parameters, r_i/r_o and b/t . As stated earlier, the closed form solutions ignore the influence of specimen width (b) on the stress state.

In light of the discussion in Section 2, the mechanics of materials solution will be compared to the FEA numerical solution.

Embree and Segall [6] used FEA to study the effect of C-ring geometry on its state of stress uniaxiality. They defined stress uniaxiality to occur when $\sigma_\theta/\sigma_z > 10$ at the center of the outer surface of the C-ring specimen at the 3-o'clock position (Fig 1). Embree and Segall performed FEA simulations using the matrix shown in Table I. The present study replicated the same simulations and expanded on their published results in the revisitation of the C-ring geometry. In all of these simulations, an outer radius of 50.8 mm and Poisson's ratio of 0.155 were kept constant, while b and r_i were varied. Furthermore, all C-ring configurations were loaded to produce the same maximum hoop stress of 100 MPa.

Figure 4 displays four of the 20 C-ring geometries considered in this study. Figure 5 shows a typical mesh distribution used to simulate the one-quarter symmetric C-ring model using Solid95 elements in ANSYS. Figure 6 displays a typical hoop stress distribution in a C-ring. It is to be noted that the maximum hoop stress occurs at the edge of the specimen - an indication the stress state is deviating from a plane stress condition.

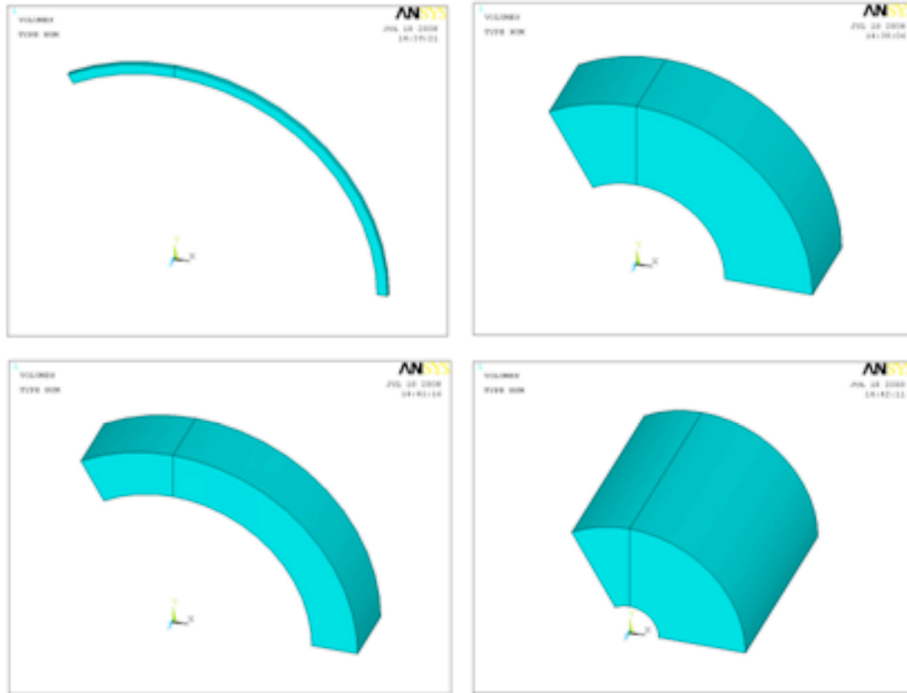


Figure 4. One-quarter symmetric model for four of the 20 C-ring geometries considered in this study. The width in the figures is half of the actual C-ring width (symmetry).

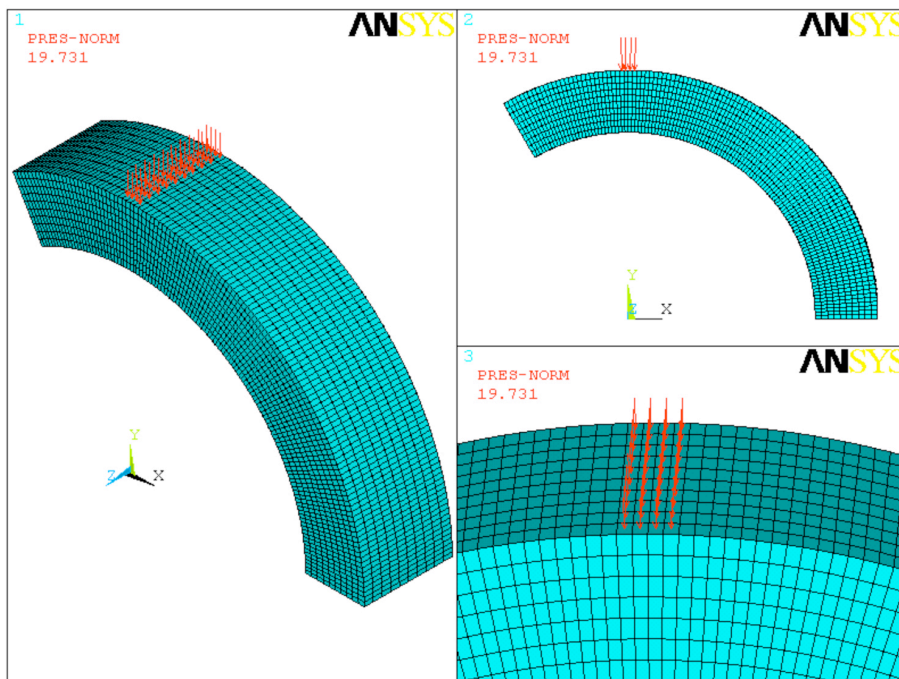


Figure 5. Mesh distribution of ANSYS Solid95 type elements.

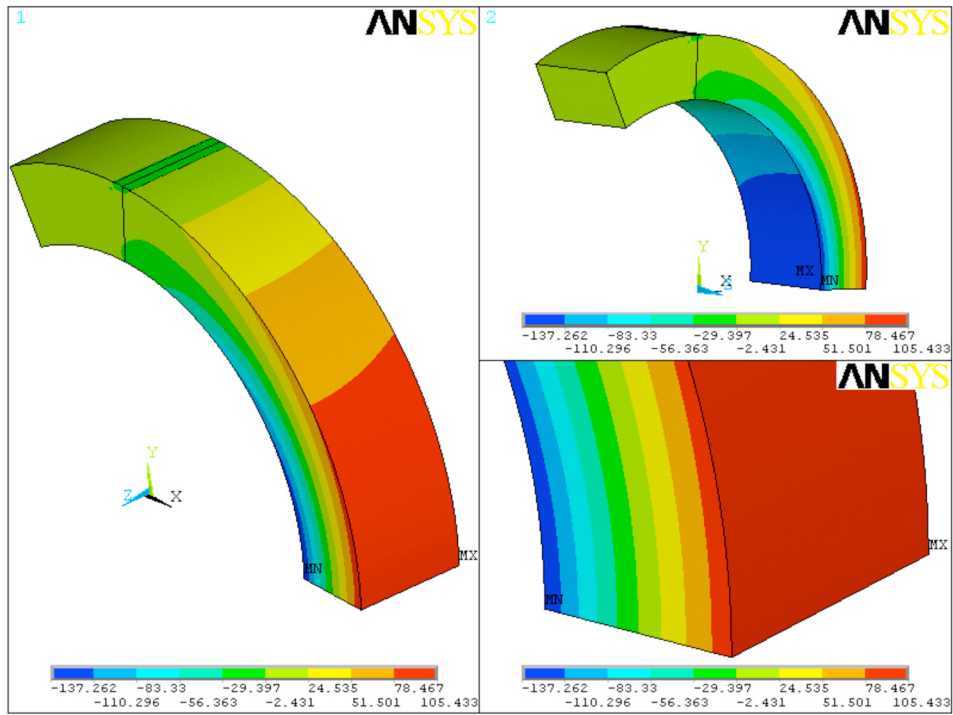


Figure 6. Hoop stress distribution in the C-ring. Note that the maximum hoop stress occurs at the edge of the specimen.

Table I. Simulation matrix and FEA results for various C-ring geometries.

| P (N) | b (mm) | t (mm) | r_i/r_o | b/t | % difference between theory and FEA | σ_θ/σ_z | $\frac{\sigma_{\theta_edge}}{\sigma_{\theta_center}}$ | Ve/V | Ae/A |
|-----------|--------|--------|-----------|-----|-------------------------------------|--------------------------|---|--------|--------|
| 60096.15 | 38.1 | 38.1 | 0.25 | 1 | -7.54 | 10754 | 1.035 | 0.0190 | 0.0966 |
| 10250.5 | 25.4 | 25.4 | 0.5 | 1 | -1.49 | -283.5 | 1.022 | 0.0163 | 0.0805 |
| 888.68 | 12.7 | 12.7 | 0.75 | 1 | -0.06 | -365.2 | 1.010 | 0.0157 | 0.0730 |
| 5.66 | 2.54 | 2.54 | 0.95 | 1 | -0.01 | -133345 | 1.002 | 0.0141 | 0.0682 |
| 120192.3 | 76.2 | 38.1 | 0.25 | 2 | -7.25 | 13.3 | 1.064 | 0.0151 | 0.0988 |
| 20501 | 50.8 | 25.4 | 0.5 | 2 | -0.15 | 26.7 | 1.066 | 0.0125 | 0.0788 |
| 1777.35 | 25.4 | 12.7 | 0.75 | 2 | 0.94 | 185.9 | 1.040 | 0.0134 | 0.0787 |
| 11.32 | 5.08 | 2.54 | 0.95 | 2 | 0.20 | -10848 | 1.008 | 0.0137 | 0.0840 |
| 180288.45 | 114.3 | 38.1 | 0.25 | 3 | -8.45 | 8.4 | 1.056 | 0.0147 | 0.1064 |
| 30751.5 | 76.2 | 25.4 | 0.5 | 3 | -0.25 | 10.2 | 1.082 | 0.0109 | 0.0763 |
| 2666.03 | 38.1 | 12.7 | 0.75 | 3 | 1.96 | 29.7 | 1.075 | 0.0109 | 0.0718 |
| 16.97 | 7.62 | 2.54 | 0.95 | 3 | 0.52 | 12435.0 | 1.018 | 0.0129 | 0.0879 |
| 240384.6 | 152.4 | 38.1 | 0.25 | 4 | -9.30 | 7.8 | 1.045 | 0.0152 | 0.1160 |
| 41002 | 101.6 | 25.4 | 0.5 | 4 | -1.20 | 7.4 | 1.073 | 0.0107 | 0.0793 |
| 3554.70 | 50.8 | 12.7 | 0.75 | 4 | 2.36 | 13.5 | 1.098 | 0.0095 | 0.0666 |
| 22.63 | 10.16 | 2.54 | 0.95 | 4 | 0.95 | 300.2 | 1.031 | 0.0120 | 0.0862 |
| 300480.75 | 190.5 | 38.1 | 0.25 | 5 | -9.61 | 7.8 | 1.040 | 0.0156 | 0.1232 |
| 51252.5 | 127 | 25.4 | 0.5 | 5 | -2.10 | 6.7 | 1.061 | 0.0109 | 0.0840 |
| 4443.38 | 63.5 | 12.7 | 0.75 | 5 | 2.00 | 8.9 | 1.100 | 0.0090 | 0.0658 |
| 28.29 | 12.7 | 2.54 | 0.95 | 5 | 1.46 | 117.9 | 1.047 | 0.0111 | 0.0816 |

* The last two columns refer to the effective volume/volume ratio and the effective area to area ratio for Weibull modulus $m=10$.

Continuing the theme of Section 1, Fig. 7 shows how the FEA solution deviates from the mechanics solution as a function of b/t and r_i/r_o . This figure is essentially a topographic map where the colors indicate the % difference between the FEA and mechanics of materials approaches as function of r_i/r_o and b/t . For example, for a C-ring specimen with $b/t = 4$ and $r_i/r_o = 0.75$, the mechanics of materials solution for the maximum hoop stress at the center of outer surface at the 3-o'clock position deviates by 2-4% (see legend) from that of the FEA simulation.

For an error less than 2%, the C-ring specimens within the purple region of Fig. 7 would satisfy that criterion. As can be seen from this figure, keeping the C-ring b/t between 1-3 and r_i/r_o between 0.50 and 0.95 would ensure that the mechanics of materials stress formula (Eq. 2) be within 2% of the FEA solution. As expected, Fig. 7 shows that as a C-ring gets wider and thicker, the FEA and mechanics solutions deviate accordingly. This is because the C-ring approaches plane strain rather than the assumed plane stress condition inherent in the mechanics of materials and elasticity theories. For example, the mechanics solution for maximum hoop stress in a C-ring with $3 < b/t < 5$ and $r_i/r_o = 0.25$ differ by 8-10% from that predicted by FEA.

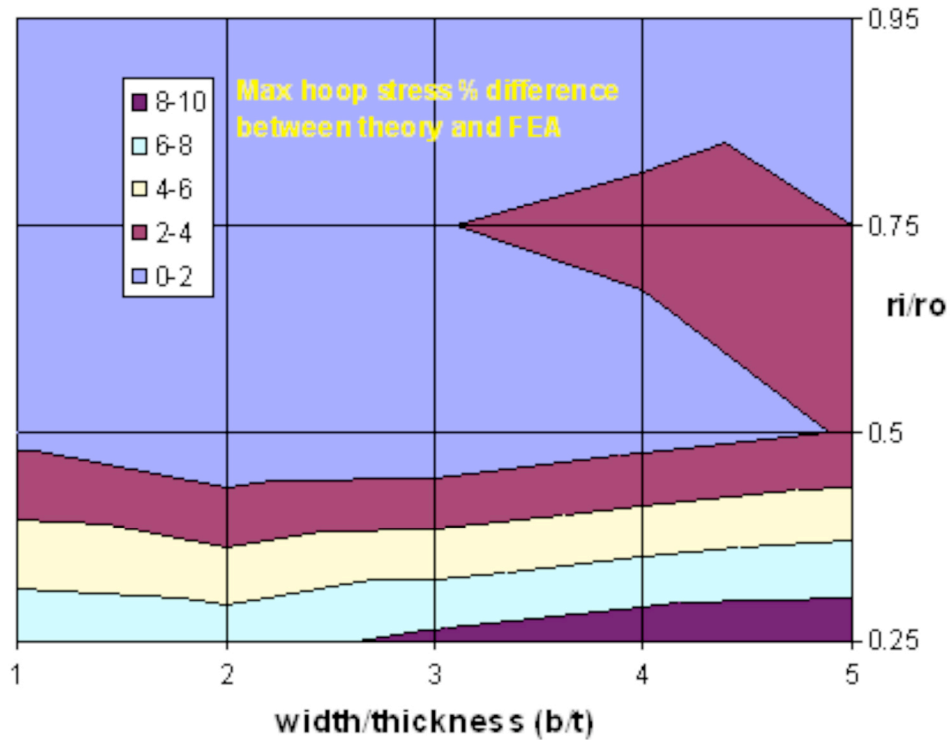


Figure 7. % difference between mechanics solution and FEA for maximum hoop stress value as function of r_i/r_o and b/t .

The ratio of the hoop stress to axial stress (σ_θ/σ_z) at the center of the outer surface at the 3-o'clock position is used to assess the uniaxiality of stress state in the C-ring specimen. As σ_θ/σ_z decreases, the C-ring specimen deviates from uniaxiality and plane stress condition and approaches that of multiaxiality and plane strain condition. A goal should be to standardize the ASTM C-ring specimen with a uniaxial stress state.

Embree and Segall [6] stated that if $\sigma_\theta/\sigma_z > 10$ then the specimen can be assumed to be in a uniaxial stress state. The present study will adopt their argument in this report. However, the results computed and included in this report are robust enough to permit changing this value and designing specimen geometries to obey whatever uniaxiality ratio one deems suitable.

Figure 8 displays a topographic map of the uniaxiality ratio as function of b/t and r_i/r_o . The computed uniaxiality ratios are widespread in this figure. In order to see the demarcation below and above the uniaxiality ratio of 10, Fig. 9 zooms in at values between -50 and 50 and clearly shows where this ratio goes below 10.

Per Fig. 9, in order to keep the uniaxiality ratio above 10, the following geometries must be maintained:

- $1 < b/t < 3$ and any r_i/r_o above 0.25,
- $3 < b/t < 4$ and $r_i/r_o > 0.50$, and
- $4 < b/t < 5$ and $r_i/r_o > 0.75$.

A union of these recommendations, and that made earlier to keep the FEA and mechanics of materials solutions within 2% of each other, leads to the same conclusion that the C-ring geometry should have its b/t between 1-3 and r_i/r_o between 0.50-0.95. ASTM C1323 presently allows for b/t to be as large as 4; the present analysis recommends that this be reduced to 3.

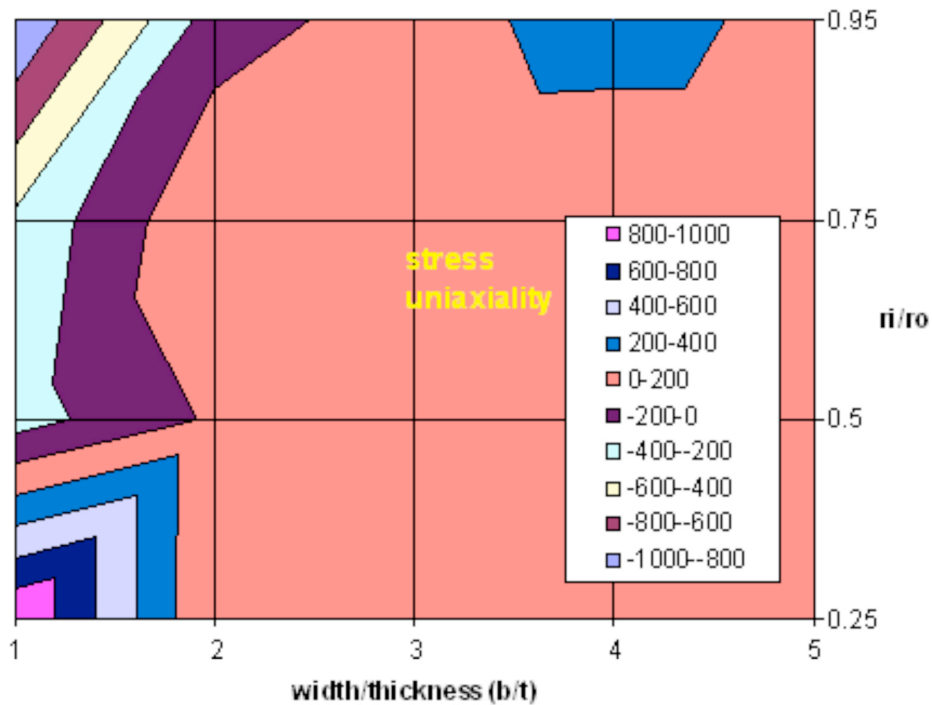


Figure 8. Stress uniaxiality ratio (σ_{θ}/σ_z) as function of b/t and r_i/r_o .

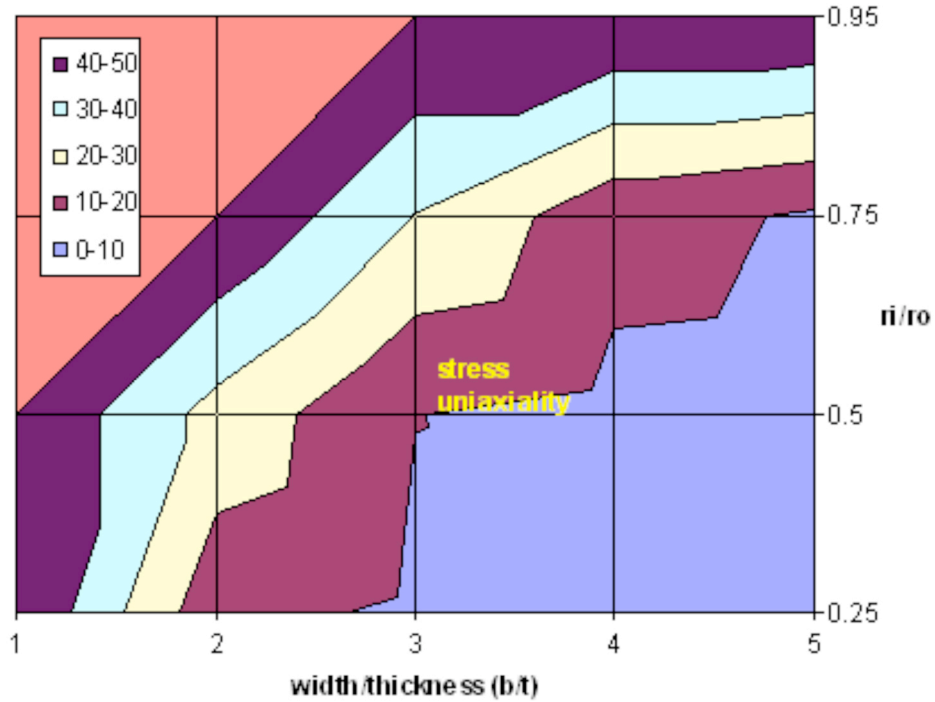


Figure 9. Absolute value of the stress uniaxiality ratio (σ_{θ}/σ_z) as function of b/t and r_i/r_o . The scale for the uniaxiality ratio is zoomed in to highlight the demarcation below and above a value of 10.

Uniformity of the hoop stress distribution along the width of the C-ring specimen is yet another parameter that can be used to assess the plane stress state in the specimen. In addition, this parameter is important because it can be used to avoid edge failures in C-rings due to significantly higher edge hoop stress. Figure 10 shows a topographic map of the ratio of edge hoop stress to center hoop stress at 3-o'clock position of outer surface as function of b/t and r_i/r_o . As can be seen from Fig. 10, if the edge stresses are to be kept low (equal to that at the center), then C-rings should tend to be narrow and thin.

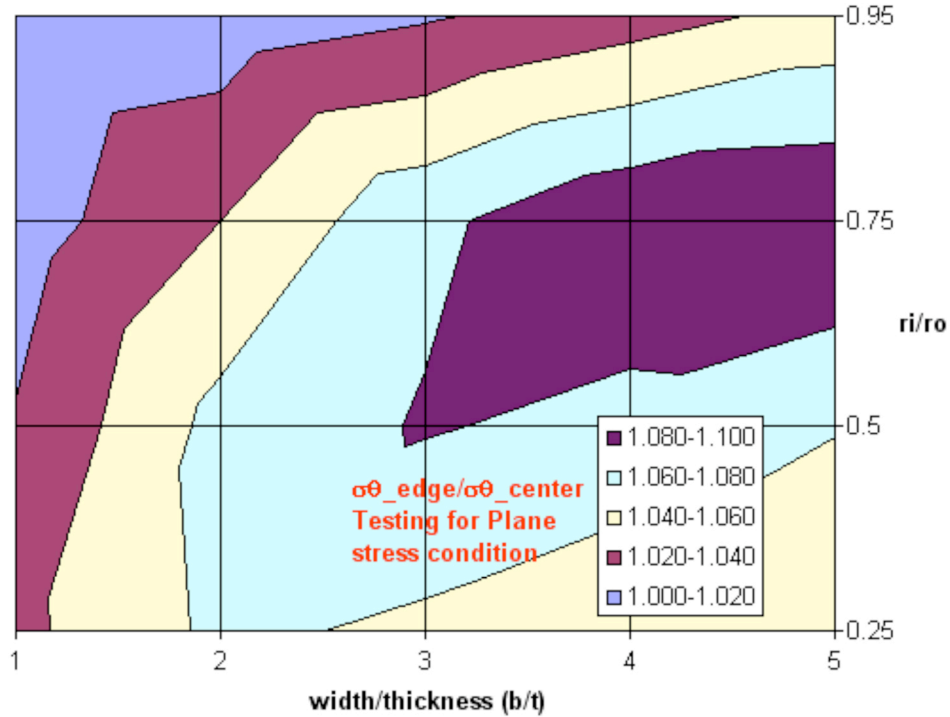


Figure 10. Ratio of edge hoop stress to center hoop stress at 3-o'clock position of outer surface as function of b/t and r_i/r_o .

4. RECOMMENDATIONS

Based on the analysis and parameters considered in the work, a C-ring specimen's geometry should be maintained within the following ranges:

$$1 \leq b/t \leq 3 \quad \text{and} \quad 0.50 \leq r_i/r_o \leq 0.95.$$

ASTM C1323 presently allows for b/t to be as large as 4; that should be reduced to 3. Of course there are stability issues with very thin specimens. These are up to the experimentalists to decide. Lastly, this investigation was performed using Poisson's ratio $\nu = 0.155$; the recommended values of b/t and r_i/r_o may change somewhat for different Poisson's ratios.

5. ACKNOWLEDGEMENTS

Research sponsored by the U.S. Department of Energy, Assistant Secretary for Energy Efficiency and Renewable Energy, Office of Vehicle Technologies, as part of the Propulsion Materials Program, under contract DE-AC05-00OR22725 with UT-Battelle, LLC. The authors thank J. -A. Wang and H. Wang for reviewing the manuscript.

6. REFERENCES

- [1] "Standard Test Method for Ultimate Strength of Advanced Ceramics with Diametrically Compressed C-Ring Specimens at Ambient Temperatures," ASTM C1323-96, Vol. 15.01, ASTM International, West Conshohocken, PA, 2008.
- [2] S. F. Duffy, E. H. Baker, A. A. Wereszczak, and J. J. Swab, "Weibull Analysis Effective Volume and Effective Area for a Ceramic C-Ring Test Specimen," *Journal of Testing and Evaluation*, 33:233-238 (2005).
- [3] S. P. Timoshenko and J. N. Goodier, *Theory of Elasticity*, McGraw-Hill, 1970.
- [4] M. K. Ferber, V. J. Tennery, S. B. Waters, and J. Ogle, "Fracture Strength Characterization of Tubular Ceramic Materials Using a Simple C-ring Geometry," *Journal of Materials Science*, 21:2628-2632 (1986).
- [5] O. M. Jadaan, D. L. Shelleman, J. C. Conway, Jr., J. J. Mecholsky, Jr., and R. E. Tressler, "Prediction of the Strength of Ceramic Tubular Components: I-Analysis," *Journal of Testing and Evaluation*, 19:181-191 (1991).
- [6] T. Embree and A. Segall, "Evaluation of the Uniaxiality of the Stress State in C-Ring Fracture Strength Specimens," *Journal of Testing and Evaluation*, 32:153-160 (2004).